ANALYTICAL PERFORMANCE EVALUATION OF HYBRID DESICCANT AIR CONDITIONING SYSTEMS

تقييم أداء تحليلي لأنظمة تكييف الهواء الثنائية التي تستخدم ماده مازه للرطوبة

A.M. Elzahaby, M. Fouad*, A.E. Kabeel, A. Khalil, and M.M. Bassuoni
Mechanical power engineering department, Faculty of engineering, Tanta University, Egypt
* Mechanical power engineering department, Faculty of engineering, Cairo University, Egypt

خلاصة:
يستعرض البحث دراسة نظرية لتقييم أداء أنظمة تكييف الهواء الثنائية لنوعين مختلفين هما النظام البعدى والنظام القبلي ، وكذلك مقارنتهما بنظام التكييف التقليدي الذي يستخدم دورة انضغاط البخار . تم دراسة أداء عجلة تجفيف الهواء الدوارة والتي تستخدم محلول كلوريد الليثوم كمادة مازه للرطوبة بوصفها قلب النظام الثنائي ولتنفيذ هذا تم وضع نموذج رياضي يصف انتقال الحرارة والكتلة داخل هذا النظام ووجد توافق جيد بين النموذج محل الدراسة وبين نموذج لباحث أخر . تم دراسة بعض العوامل التي تؤثر على أداء النظام منها: سرعة دوران عجلة التجفيف ، عدد الوحدات المنقولة ، مساحة سطح المادة المازه بالنسبة الى حجمها ، درجة حرارة وسرعة هواء التنشيط ، قطر مجرى الهواء داخل عجلة التجفيف ، فاعلية المبخر والمكثف وكذلك فاعلية عجلة التجفيف . وجد من الدراسة أن نظام تكييف الهواء الثنائي البعدى يوفر قدرا مناسبا فى سعة ملف التبريد يصل إلى 30% مقارنة بالنظام التقليدي ويصل معامل أداء هذا النظام الى ضعف قيمة معامل أداء النظام التقليدي باستخدام سخان طرفي . أما فى نظام تكييف الهواء القبلي فقد وجد أنه يحقق أقل درجة حرارة ندى لهواء التغذية (تصل إلى6°C) مع وجود زيادة فى معامل أداء هذا النظام تصل إلى 80% مقارنة بالنظام التقليدي باستخدام سخان طرفي .

Abstract

A theoretical evaluation of a hybrid desiccant air conditioning in post and pre-cooling arrangements is studied and compared versus the traditional vapor compression system (VCS). The performance of the rotary desiccant wheel is also studied as the heart of the hybrid desiccant cooling system. Lithium chloride is applied as the working desiccant material in this investigation. A mathematical model of coupled heat and mass transfer of the desiccant wheel is presented and numerically solved. The model validity is checked against other work and results are in good agreement. Effects of rotary wheel speed, number of transfer units (NTU) and the desiccant surface area to volume on the performance of the wheel are investigated. The effect of regeneration air velocity and temperature, slot diameter, evaporator and condenser effectiveness and dehumidification effectiveness on the system performance is also studied. The post cooling hybrid system is found to be an energy efficient system, it saves up to 30% of cooling coil capacity compared to traditional VCS. The COP of the post cooling arrangement is nearly twice that of VCS with reheat. The pre cooling arrangement supplies air at lower dew point temperature (down to 6°C) with an increase of COP up to 80% compared to VCS with reheat.

Keywords: hybrid desiccant system; vapor compression system; rotary desiccant wheel.

Nomenclature

C_P	Specific heat at constant pressure, J/kg.K.	f	Desiccant surface area to volume ratio, m^2/m^3
D_s	Surface diffusivity of desiccant, m^2/s	h	Enthalpy, J/kg
d	diameter, m	K	Mass transfer coefficient ,$kg/m^2.s$

Accepted September 24, 2008

L	Wheel thickness, m
M	mass per unit volume, kg/m^3
$\dot{m}$	Mass velocity, $kg_{dry\ air}/m^2.s$.
p	Pressure, Pa
q	Heat of absorption, J/kg_{water}
Q	Heat transfer rate, kW
T	Temperature, °C
t	Time, s
w	Desiccant moisture content, $kg_w/kg_{desiccant}$
W	Power consumption, kW
X	Wheel desiccant concentration, $kg_{desiccant}/kg_{sol}$
Y	Air humidity ratio kg_{vapor}/kg_{air}

Greek

ε	Void fraction (-)
α	Heat transfer coefficient, W/m^2.K.
λ	Thermal conductivity of desiccant, W/m.K
ρ	Density, kg/m^3
ε_d	Dehumidification effectiveness, (-)
ε_{ev}	Evaporator effectiveness, (-)
ε_{sx}	Sensible HX effectiveness, (-)
ϕ	Fraction of inert material, (-)
ψ	Thermal capacitance ratio, (-)
η	Efficiency
μ_a	Air dynamic viscosity, Pa.s
ε_{cond}	Condenser effectiveness, (-)

Abbreviations

NTU	Number of transfer units, (-)
Re	Reynolds number.
SHX	Sensible heat exchanger.
SMRR	Specific moisture removal rate, g/kg.s

Subscripts

a	Air
abs	Absorption
avg	Average value
cc	Cooling coil
D	Desiccant
L	Liquid
reg	Regeneration
S	Supporting structure
V	Vapor

1. Introduction

Nearly thirty percent of the primary energy resources are consumed in the air conditioning sector. The primary energy shortage, negative environmental impacts of fossil fuels and bad indoor air quality (IAQ) of traditional systems are the main incentives for developing air conditioning techniques which can either save energy or employ low grade thermal energy sources. Among various techniques actively used currently, hybrid desiccant cooling is a promising choice [1]. In the mid of 1960's Dunkle [2] proposed a method of air conditioning which was driven principally by solar rather than electrical energy. His system uses a desiccant for dehumidification along with evaporative coolers and heat exchangers for sensible cooling. This concept has much research into developing a desiccant air conditioning system for residential use however very little work has been done to apply the desiccant concept to commercial sized buildings. Close and Sheridan [3] extended the use of residential desiccant system to meet commercial sized cooling loads. Sheridan and Mitchell [4] examined the use of commercial sized hybrid solar desiccant cooling system in Australian climates. Their study showed great promise for an air conditioning system which combines the technology of a vapor compression system with the advanced concept of desiccant dehumidification. They investigated the performance of a hybrid desiccant cooling system for hot-humid and hot-dry climates. At high sensible heat load, SHF was over 0.9 while at high latent load, SHF

varied from 0.3 to 0.5. In high sensible heat load applications the energy savings ranged from 24 to 40% for these two climates. However, they also found that the hybrid cycle saved more energy in a hot and dry climate than it did in a hot and humid climate, where it may even use more energy than a conventional system. Robert [5] introduced a commercial hybrid air conditioning system. He concluded that the hybrid system reduces the compressor work of the mechanical refrigeration unit from 55–70% compared to the conventional vapor compression system. And the net effect of the electrical energy reduction is in order of 40–50%. Burns et al. [6] studied three hybrid system configurations for supermarket applications (high latent load) and a comparison of their performance with conventional air-conditioning system was made. The cycles termed as ventilation-condenser cycle, recirculation-condenser cycle and ventilation-heat exchanger cycle. They reported that these cycles would give energy savings, in comparison to the conventional air-conditioning systems, ranging from 56.5 to 66% at moderate ambient conditions of 30°C, 0.016 $kg_{vapor}/kg_{dry\ air}$, SHF of 0.35 and space conditions of 24°C, 0.0104 $kg_{vapor}/kg_{dry\ air}$. These calculations were based on the concept of weighted energy consumption, with one unit of electrical energy weighted twice that of thermal energy. Maclaine-Cross [7] studied the feasibility of gas fired hybrid desiccant cooling systems for medium to large general air conditioning projects. It was suggested that engine drive for vapor compression plant could halve the energy costs for Australian conditions if waste heat was recovered to regenerate the desiccant.

Worek and Moon [8] investigated the performance of a first generation prototype desiccant integrated hybrid system. The results showed that at the same level of dehumidification, 60% performance improvement over vapor compression system was obtained at ARI design conditions (for outdoor air, Tdb=35.0°C and RH=40%; for room air, Tdb=26.7°C and RH=50%). The performance of hybrid system decreased as the outdoor humidity ratio was increased. Nevertheless, over the range investigated, the performance improvement varied from 74 to 44%.

Singh et al. [9] have analyzed the afore-mentioned three hybrid cycles, introduced in [6], for Indian climatic conditions. Modeling of the dehumidifier operating at a fixed regeneration temperature of 135°C, and regeneration to process air mass flow ratio of 0.33, is done using the performance data from a manufacturer. It is reported that energy savings ranging from 30% to 50% can be easily achieved at higher latent heat load applications. Vazirifard et al [10] studied a possibility of using hybrid desiccant cooling systems instead of conventional vapor compression cooling systems through some key variables. These key variables can be determined if a special building in an area needs a more detailed consideration. Based on the information presented here, it appears that a high potential exists for using hybrid desiccant systems in Iran, suggesting opportunities for importing the technology, or for development of equipment locally. Mohan et. al [11] studied the performance of absorption and

regeneration columns for a liquid desiccant vapor compression hybrid system. The liquid desiccant is used only for dehumidification of supply air in the absorber which can be subsequently regenerated in the regenerator using condenser heat. They reported that higher the specific humidity and lower the temperature of the inlet air, higher will be the dehumidification in the absorber. Similarly, the regeneration can be increased by increasing the temperature and decreasing the specific humidity of the inlet air to the regenerator. Further, the solution temperature has negligible effect on the performance of air dehumidification or solution regeneration owing to low flow rate of the solution.

In this paper a theoretical evaluation of two different arrangements of the hybrid desiccant system versus traditional systems is presented. Also, a mathematical model of coupled heat and mass transfer of the desiccant wheel is developed and numerically solved. This model is validated by comparing it with other models [12]. Effects of rotary wheel speed, number of transfer units (NTU) and the ratio of desiccant surface area to volume on the performance of the wheel are also investigated in this work.

2. The Hybrid System

The hybrid desiccant system consists mainly of a vapor compression cycle (DX type) and a rotating desiccant wheel. The desiccant wheel geometry is shown in Fig.1. The honeycomb rotor consists of *N* identical narrow straight cylindrical slots uniformly distributed over the cross sectional area of the rotor.

In the post-cooling hybrid desiccant system shown in Fig. 2(a), air is dehumidified in the

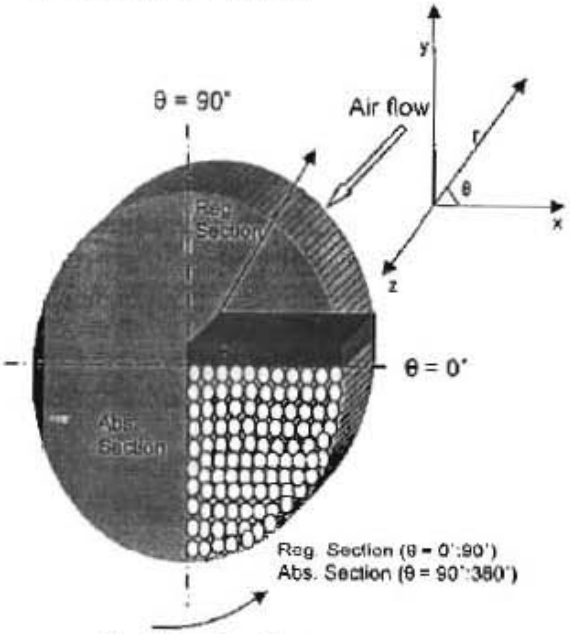

Fig. 1 Desiccant wheel geometry.

desiccant wheel (A) before it enters the cooling coil of the DX unit. The dehumidified air is then cooled in a rotary sensible heat exchanger (SHX) (G) by return air; then air is further cooled to the desired conditions by the cooling coil (B). The desiccant wheel is regenerated by the return air after it passes through the rotary heat exchanger; and further heated using an auxiliary heater (F). The psychometric chart of this model is shown in Fig. 3(a).

In the pre-cooling hybrid desiccant system shown in Fig. 2(b), air is passed through cooling coil (B) and then through the desiccant wheel (A) to reach the supply air conditions. The reactivation of the wheel is achieved by the condenser of the DX unit (H). The psychometric chart of this model is shown in Fig. 3(b). There are two processes in this figure (process 1-8-4 and 1-2-

3). The first process (1-8-4) ensures fair comparison between the post and pre-cooling systems. This is because the two systems operates at the same inlet and outlet states of the conditioned space. On the other hand, the second process (1-2-3) is used to ensure lower humidity levels as discussed later.

Because of geometric similarity of the desiccant wheel, the multiple annular layers of straight slots in the dehumidification and the regeneration sections can be replaced by a "representative annulus" of thickness Δr. The three cylindrical coordinates (r,θ,z), say radial, angular and axial directions, respectively, in the model can rationally be reduced to the two coordinates (θ,z). By taking into account the geometry of the wheel each constituent element within the total M identical elements in the θ-direction spanning the entire cross section of the representative annulus, the remaining space variable is z. Of course a second independent variable in the model is the time t. In other words the dynamic behavior of the honeycomb rotor can be simulated by following the transient changes occurring in the z-direction within each of the N slots as the rotor slowly turns. For the derivation of the governing equations of desiccant wheel, some assumptions are considered [13]. Air flow is uniformly distributed over the dehumidification and regeneration sections. No leakage takes place between dehumidification and regeneration sections. Heat and mass transfer in the radial direction is not taken into consideration as the air stream flowing through each slot is assumed to be plug or piston flow. Thermal conductivity and diffusivity of the desiccant material are isotropic. Shell of the desiccant wheel satisfies the insulated conditions. The absorption and regeneration processes through the wheel are considered adiabatic. The thermal and physical properties of air and desiccant material don't change in the range of operating temperatures. The bulk air streams contain only one absorbable component, water vapor.

The surface diffusivity is considered in the presented model of this study. This leads to an average enhancement of about 3% in the system performance rather than [13].

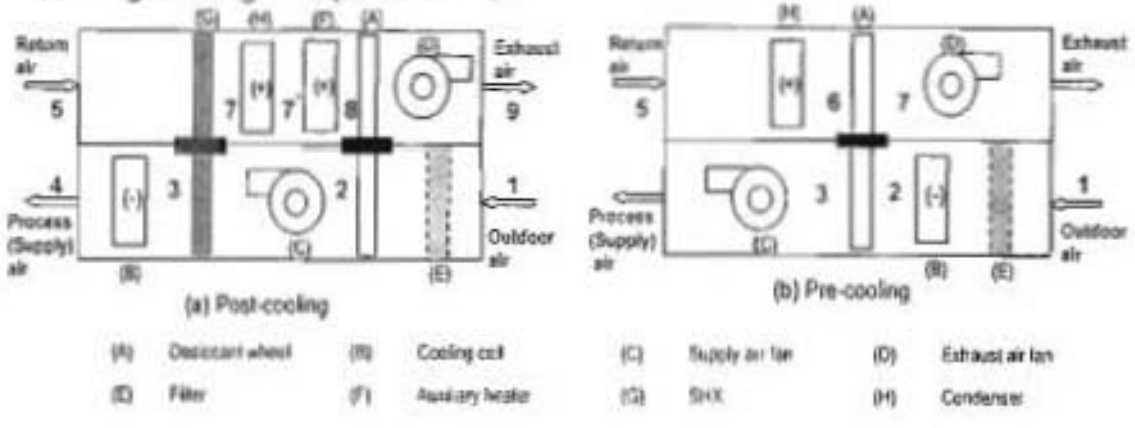

Fig. 2 A schematic of a hybrid desiccant system uses 100% FA

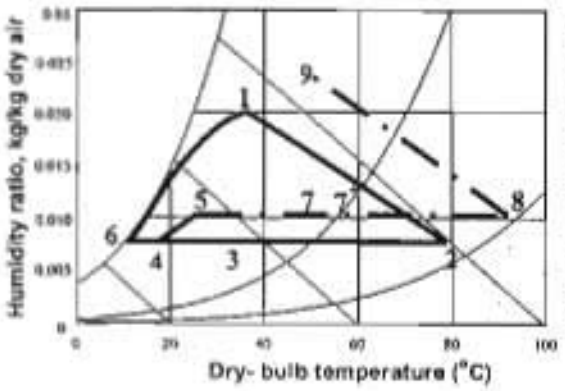

1-2 Dehumidification Process.
2-3 Cooling Process (rotary HX).
3-4 Cooling coil.
4-5 SHF (Load line).
5-7 Heat recovery (HX).
7-8 Additional heating.
8-9 Regeneration process.
1-6-4 VCS with reheat.
1: Outdoor air conditions.
4: Supply air.
5: Indoor conditions (Return air).

(a) Post cooling

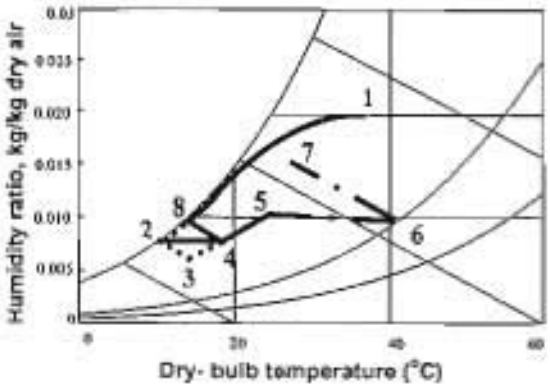

1-2 Cooling Process.
2-3 Dehumidification Process.
5-6 Heating air for regeneration.
6-7 Regeneration process.
1-2-4 VCS with reheat.
3-5 SHF(Load line).
1 Outdoor air conditions.
3 Supply air.
5 Indoor conditions (Return air).

(b) Pre-cooling
Processes (1-8-4)&(1-2-3)

Fig.3 Psychometric process for hybrid desiccant system (values shown are typical).

3. Governing Equations of the Desiccant Wheel

Based on the above considerations, the governing equations for heat and mass transfer in the rotary desiccant wheel are presented below.

Moisture and energy conservation of process air

$$\frac{\partial Y}{\partial t} + \frac{\dot{m}_a}{\rho_a \varepsilon}\frac{\partial Y}{\partial z} = \frac{K f_s}{\rho_a \varepsilon}(Y_D - Y) \quad (1)$$

$$\frac{\partial T}{\partial t} + \frac{\dot{m}_a}{\rho_a \varepsilon}\frac{\partial T}{\partial z} = \frac{\alpha f_s}{\rho_a \varepsilon (C_{pa} + Y C_{pv})}(T_D - T). \quad (2)$$

Moisture and energy conservation of absorbent

$$\frac{\partial W_D}{\partial t} - D_s(1-\varepsilon)\frac{\partial^2 W_D}{\partial z^2} = \frac{K f_s}{M_D}(Y - Y_D) \quad (3)$$

$$\frac{\partial T_D}{\partial t} - \frac{\lambda(1-\varepsilon)}{M_D(C_{PD} + W_D C_{PL}) + M_S C_{PS}}\frac{\partial^2 T_D}{\partial z^2} = \frac{\left[\alpha f_s (T - T_D) + K f_s (Y - Y_D) Q\right]}{M_D(C_{PD} + W_D C_{PL}) + M_S C_{PS}} \quad (4)$$

In the above four equations there are five unknowns; Y, Y_D, T, T_D and W_D. So, to solve them the following auxiliary relations are needed to calculate the humidity ratio near the surface of absorbent (Y_D). The humidity ratio near the desiccant surface and the desiccant concentration (X) can be evaluated from [13]

$$Y_D = \frac{0.622 P_v}{1.0133 \times 10^5 - P_v} \quad (5)$$

$$X = \frac{1}{1 + W_D} \quad (6)$$

The coefficients of mass and heat transfer are given below [14]

$$K = 0.704 \dot{m}_a \mathrm{Re}^{-0.51} \; ; \mathrm{Re} = \frac{\dot{m}_a d_{slot}}{\mu_a} \quad (7)$$

where d_{slot} is the slot diameter and μ_a is dynamic viscosity of air

$$\alpha = 0.671 \dot{m}_a \mathrm{Re}^{-0.51} C_{pa} \quad (8)$$

The absorption heat and surface diffusivity can be calculated from [14]

$$Q = \begin{cases} -1.34\times10^5 W_D + 3.5\times10^6, & W_D \le 5.0 \\ -1.4\times10^4 W_D + 2.95\times10^6, & W_D \ge 5.0 \end{cases} \quad (9)$$

$$D_s = a \times \exp\left[-0.974\times10^{-3} \frac{Q}{T_D + 273.15}\right] \quad (10)$$

$$a = 0.8\times10^{-6}$$

4. Governing Equations for the Vapor Compression System

For the traditional VCS the evaporator temperature is assumed to be 5°C less than the minimum temperature of the supply air. The condenser temperature is assumed to be 20°C higher than the outdoor air temperature. The refrigerant used is R134a; the refrigerant leaves the evaporator and condenser in saturated vapor and saturated liquid. The compression process is polytropic. The supply air leaves the cooling coil as saturated air. The evaporator and condenser exit temperatures are calculated as follows.

$$T_4 = T_3 - \varepsilon_{ev}(T_3 - T_e) \quad (11)$$

$$T_c = T_{amb} + 20 \quad (12)$$

$$T_{out} = T_{in} + \varepsilon_{cond}(T_c - T_{in}) \quad (13)$$

The actual work of the compressor can be calculated from the polytropic work relation as follow

$$W_c = \frac{n P_e v_1}{n-1}\left[\left(\frac{P_{cond}}{P_e}\right)^{\frac{n-1}{n}} - 1\right] \times \frac{1}{\eta_C \eta_m \eta_e} \quad (14)$$

Where η_c is the compressor isentropic efficiency, v_1 is the specific volume of the saturated vapor refrigerant, p_{cond} is the condenser saturation pressure, p_{ev} is the evaporator saturation pressure, W_c is the actual compressor work and η_m, η_e are the mechanical and electrical efficiencies, respectively.

From psychometric chart shown in Fig. 2(a) the temperature at exit from the sensible heat exchanger can be calculated as follows:

$$T_7 = T_5 + \varepsilon_{HX}(T_2 - T_5) \quad (15)$$

$$T_3 = T_2 - \frac{\dot{m}_5}{\dot{m}_2}(T_7 - T_5) \quad (16)$$

5. Hybrid System Performance Analysis

The following coefficients are used to measure the hybrid desiccant cooling system performance, refer to Fig.3(a) for post-cooling arrangement.

$$ECOP = \frac{Q_L}{W} \quad (17)$$

where $ECOP$ is the hybrid system coefficient of performance, Q_L is the specific cooling capacity including desiccating and heat recovery and W is the total power consumption.

$$Q_L = \dot{m}\left[(h_1 - h_2) + (h_2 - h_3) + (h_3 - h_4)\right] = \dot{m}(h_1 - h_4) \quad (18)$$

$$W = W_c + W_{fans} + W_{AH} \quad (19)$$

where W_{fans} is the fans power consumption, W_{AH} is the auxiliary heat for regeneration in (kW) and calculated from

$$W_{AH} = \dot{m}(h_8 - h_{7'}) \quad (20)$$

Here, one kW of electrical energy is equal to three kW of thermal energy.

$$VCOP = \frac{Q_{cc}}{W_c} \quad (21)$$

where $VCOP$ is the vapor compression cycle COP and Q_{cc} is

the cooling coil load without desiccating and is calculated from

$$Q_{cc} = \dot{m}\,(h_3 - h_4) \tag{22}$$

The above mentioned equations can be applied for the pre-cooling arrangement by referring to Fig. 3(b) with some little change.

The specific enthalpy (h) of the air is calculated from:

$$h = 1.005T + Y(2501 + 1.805T) \tag{23}$$

where Y is the humidity ratio of air and T is the air temperature. The specific moisture removal rate ($SMRR$) is calculated from

$$SMRR = \frac{\dot{m}(\Delta Y)}{m_d} \tag{24}$$

where $\dot{m}$ is the mass flow rate of air, ΔY is the specific humidity drop in process air and m_d is the mass of the desiccant material which calculated from

$$m_d = \frac{\pi}{4} \times D_{wheel}^2 \times M_D \times (1-\varepsilon) \times (1-\phi) \times L \tag{25}$$

The dehumidification effectiveness (ε_d) is calculated from

$$\varepsilon_d = \frac{\Delta Y}{Y_{in}} \tag{26}$$

where D_{wheel} is the desiccant wheel diameter and ϕ is the fraction of inert material. The number of transfer units (NTU) is calculated from

$$NTU = \frac{KA_s}{\dot{m}} \tag{27}$$

where A_s is the total surface area of the desiccant material which is calculated from

$$A_s = f_v \times V_D \,,\qquad f_v = \frac{4 \times \varepsilon}{d_{pore} \times (1-\varepsilon) \times (1-\phi)} \tag{28}$$

where f_v is the desiccant surface area to volume ratio and V_D is the volume of the desiccant material.

The thermal capacitance ratio of the wheel is

$$\psi = \frac{m_d C_{PD}}{m_s C_{PS}} \tag{29}$$

The boundary and initial conditions for the differential equations (1)-(4) for both regeneration and absorption processes are introduced according to whether the system is post or pre-cooled. These equations are discretized using fully implicit scheme for time varying terms and upwind difference scheme for space varying terms. These equations are solved using tri-diagonal matrix technique (TDMT) using a computer code written in Matlab.

6. Model Validation

The validation of the mathematical model that describes the mass and heat transfer through the absorption and regeneration processes in the desiccant wheel is performed by comparing these results with that of [12] using R.D silica gel as a desiccant material. The cycle time of the rotary wheel is 512 second, the regeneration cycle time is 256 second i.e. the regeneration to absorption area ratio is unity. As shown in Fig. 4a, the numerical results of the present model are compared with that of [12]. The comparison shows a reasonable agreement with the two numerical results in the order of 1.6% average. Also, from Fig.4b The comparison between measured data and calculated results for the ECOP at different rotational speed shows a reasonable agreement between the measured data and calculated results. The difference is in order of 1 to 5%; this may emphasize the validity of the model to predict the performance of the hybrid system. The difference may be due to the

assumptions of the theoretical model and also, the accuracy of the measurements.

7. Discussion and Analysis

The performance investigation of the desiccant wheel at different parameters to obtain the best values for operation is performed. The effects of rotational speed, NTU, the desiccant surface area to volume ratio, thermal capacitance ratio and regeneration to absorption area ratio are studied. On the other hand a comparison between the different arrangements of the hybrid desiccant cooling system and VCS is also introduced at different operating and design parameters.

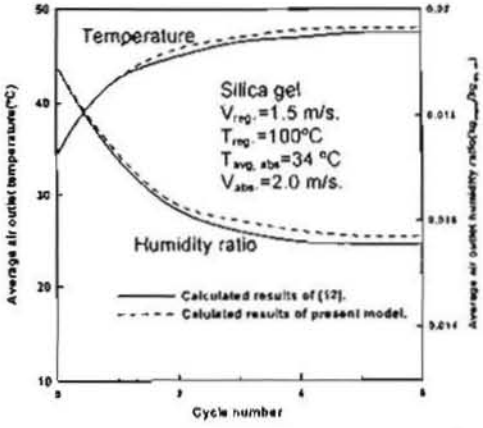

Fig. 4a Average air exit temp and humidity ratio of process air obtained from [12] and the present study.

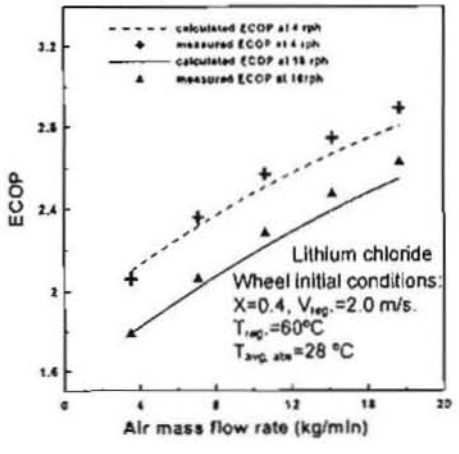

Fig. 4b Comparison between the ECOP of calculated and measured data of present study.

7.1 Desiccant Wheel Performance Analysis

7.1.1 Effect of Rotational Speed

Figure 5 shows the variation of dehumidification performance measures ε_d and SMRR of the desiccant wheel with rotational speed at different regeneration velocities. There exists an optimum speed very close to 1 rph at which the dehumidification performance and the specific moisture removing rate reaches maximum values. By increasing the rotational speed from 0.2 to 1.2 there are an observed increasing up to 0.5 for ε_d and 0.32 for SMRR. By exceeding the rotating speed beyond 8 rph, the values of ε_d and SMRR are decreasing rapidly to attain the lowest values of 0.23 and 0.1 respectively. When the desiccant wheel rotates faster than the optimum value, the time of absorption and regeneration processes are too short which results in decreased ε_d and SMRR. On the other hand, when the rotary speed is lower than the optimum, the time of absorption and regeneration processes are too long and wasting more energy in sensible heating for regeneration and sensible cooling for absorption. The increasing of the velocity and temperature of the regeneration air enhances the dehumidification performance of the desiccant wheel. This is because the efficiency of regeneration process is improved by increasing the regeneration air velocity and temperature as shown in Fig. 6. It is very important to use the suitable temperature and velocity for regeneration to save energy consumption. From Fig. 6 the energy required for regeneration process at (V_{reg}= 4m/s and T_{reg}=

70°C) is 1.18 kW and that at (V_{reg}= 4m/s and T_{reg}= 60°C) is 0.52 kW.

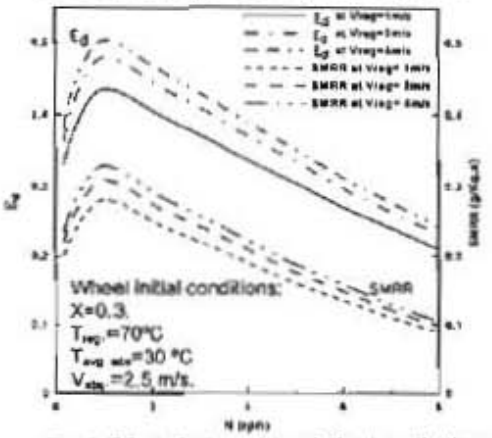

Fig. 5 Effect of rph on dehumidification effectiveness.

7.1.2 Effect of Number of Transfer Units

Figure 7 shows the effect of number of transfer units (NTU) on the dehumidification performance. The NTU has a great influence on the performance. When the wheel mass and slot diameter are fixed, the NTU will increase with the increase in the wheel thickness. When the NTU increases from 0 to 2.5, both SMRR and ε_d increases rapidly, however when the NTU is larger than 2.5 there is a little increase in the performance, so a value of NTU of 2.5 may be considered as a suitable one to perform well . This may be because the increase of NTU over 2.5 requires more regeneration heat as a result of wheel volume increase. Resulting in increasing the regeneration temperature to sustain the increase in the wheel volume and remove the amount of moisture absorbed from air. Note that increasing NTU may also increase the pressure drop across the wheel slightly.

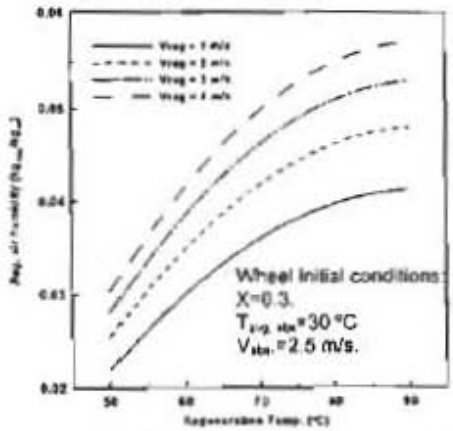

Fig. 6 Effect of regeneration temp. on the regeneration air exit humidity ratio.

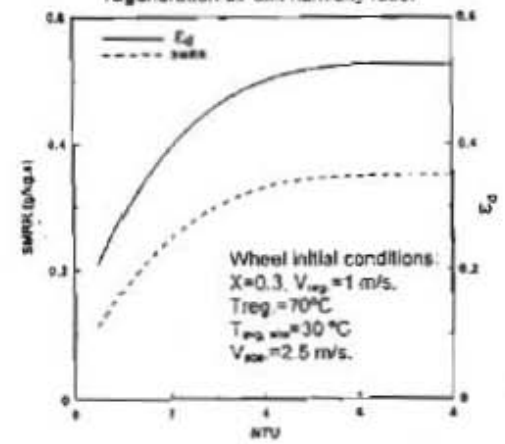

Fig. 7 Effect of NTU on dehumidification performance.

7.1.3 Effect of Desiccant Surface Area to Volume Ratio f_v

Figure 8 shows the effect of desiccant surface area to volume ratio f_v on the dehumidification performance. When the total volume of the wheel is fixed, higher contact area of mass and heat transfer can be achieved by constructing smaller slots with thinner wall. With higher values of f_v the desiccant wheel will be more efficient as the mass transfer area become larger, so higher values of f_v are recommended. A typical value of f_v is 1500 m^2/m^3 at NTU of 2.5. On the other hand, this will increase the fan power consumption as the pressure drop through the wheel increases.

7.1.4 Effect of Thermal Capacitance Ratio ψ

Figure 9(a) and (b) show the effect of thermal capacitance ratio ψ on the exit temperature and humidity of the process air. It can be

observed that the process air stream exits at lower temperature and with slightly higher absolute humidity as the capacitance ratio increases. This will cause a dehumidification process with less sensible heating which resulting in higher cooling capacity and considerable energy saving. The capacitance ratio increases by using an inert material (of supportive structure) with low heat capacity, or very light weight. For very light weight or low heat capacity of the supportive structure, the wheel can be easily regenerated and the air is dehumidified more efficiently. Also, the amount of heat exchanged between the regeneration and absorption sections due to rotation is minimized. The typical value of ψ is 4.

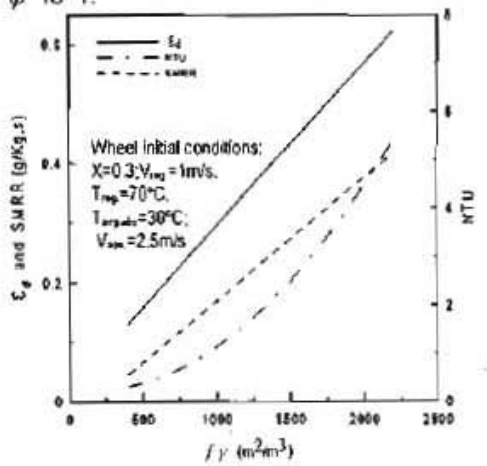

Fig. 8 Effect of desiccant surface area to volume ratio on Dehumidification performance

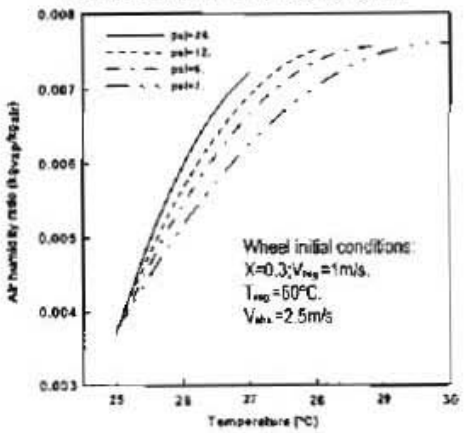

Fig. 9(a)

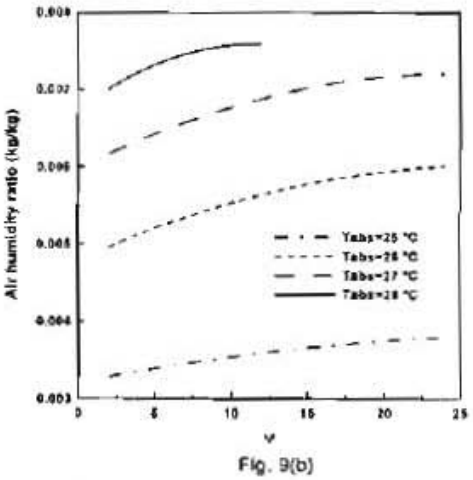

Fig. 9(b)

Fig. 9 Effect of thermal capacitance ratio ψ(psi)on process air exit humidity ratio and temperature

7.1.5 Effect of Regeneration to Absorption Area Ratio

Figure 10 shows the effect of regeneration to absorption area ratio on the SMRR of process air stream and exit humidity ratio of the regeneration air stream at a regeneration air temperature of 80°C and 60°C. The SMRR and exit humidity from the regeneration section increases to a maximum value at a regeneration to absorption area ratio of 0.33 (regeneration face area of 0.25 of the total wheel face area) at a temperature of 80°C. At a temperature of 60°C the regeneration to absorption area ratio becomes 1 (regeneration face area of 0.5 of the total wheel face area) to achieve best performance. For a small regeneration area the wheel requires more regeneration energy, when the regeneration velocity is constant, the regeneration temperature will increase. The regeneration temperature increases with the decrease of regeneration area.

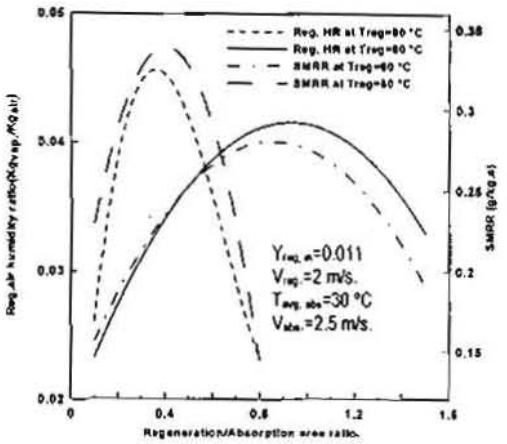

Fig. 10 Impact of regeneration / absorption area ratio on the exit humidity ratio and SMRR of the regeneration air stream.

7.2 Hybrid Desiccant System Performance Analysis

7.2.1 Impact of Slot Diameter

Figures 11(a) and (b) show the impact of slot diameter on the variation of ECOP for both post and pre-cooling arrangements. The ECOP increases with the narrow slots because the smaller the diameter of slot the larger the surface area of mass and heat transfer, which improve the dehumidification process. At a typical value of (f_v =1500m^2/m^3) the slot diameter will be 0.003m. At these values the ε_d and SMRR are 0.42 and 0.28 g/kg.s respectively. As the dehumidification process is enhanced, the latent load removed by the wheel increases and therefore increasing ECOP. The decrease in slot diameter should be limited as the fan power increases at small slot diameter as the pressure drop in the flow direction increases.

7.2.2 Impact of Dehumidification Effectiveness ε_d

Figures 12(a) and (b) show the Impact of Dehumidification effectiveness ε_d on the ECOP for

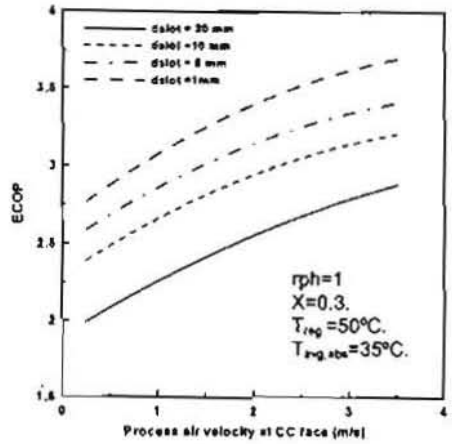

(a) Post-cooling

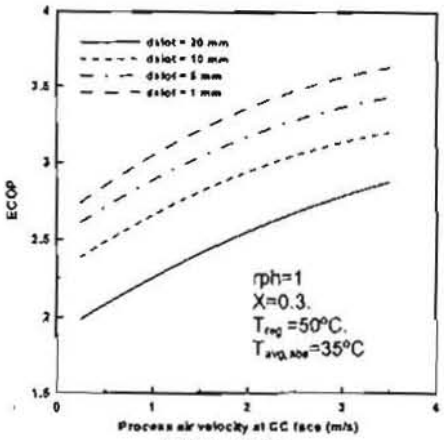

(b) Pre-cooling

Fig.11 Impact of slot diameter on ECOP

both post and pre-cooling arrangements. As the dehumidification effectiveness increases, the system ECOP is rapidly increased. This is because the higher the ε_d the higher the latent cooling capacity gained by the desiccant wheel. The typical values of ε_d is 0.4 to 0.55. The design parameters of the desiccant wheel strongly affects the dehumidification effectiveness as discussed earlier. At a typical value of (f_v =1500 m^2/m^3) and a slot diameter of 0.003 m, the value of ε_d is 0.42 . At these values the ECOP is 2.9 and 2.6 for post and pre-cooling, respectively.

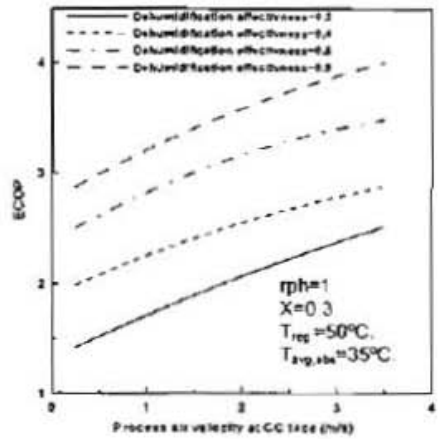

(a) Post-cooling

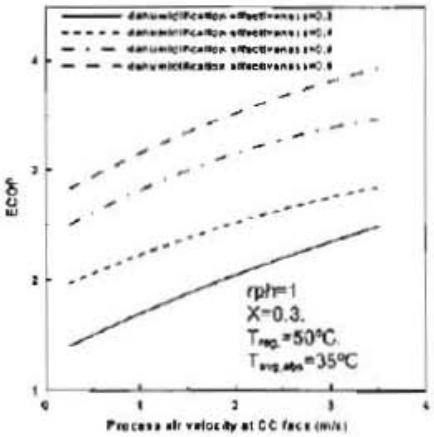

(b) Pre-cooling

Fig.12 Impact of dehumidification effectiveness on ECOP

7.2.3 Impact of Wheel Void Fraction Area (ε) and f_v

Figures 13(a) and (b) show the effects of desiccant wheel area void fraction ε and desiccant surface area to volume (f_v) on system ECOP for both post and pre-cooling arrangements. As the wheel void fraction area increases the ECOP decreases rapidly at ε value higher than 0.4. This is due to the higher values of ε that means that the desiccant material in the wheel is not sufficient to perform well. So the dehumidification process is bad, i.e. low latent load removed by the wheel and the system performance decreases. The values of ε lower than 0.4 means condensed wheel by desiccant material and at all values of desiccant surface area to volume the ECOP is slightly increased by about 8.3%. This is because increasing of f_v with the same regeneration energy will lead to slight enhancement in the dehumidification process. Also, the increasing of fan power required to overcome the wheel pressure drop.

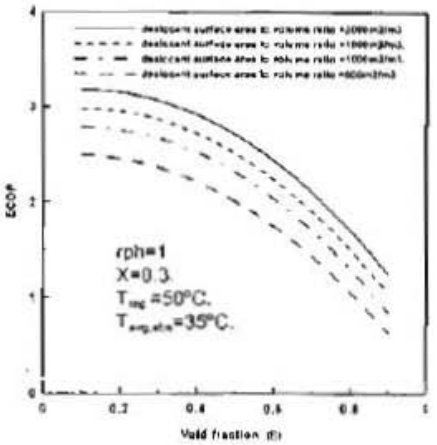

(a) Post-cooling

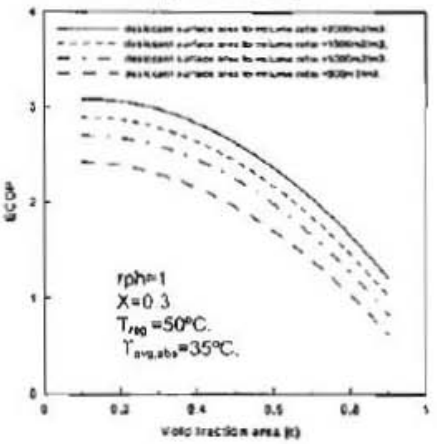

(b) Pre-cooling

Fig.13 Impact of void fraction area on ECOP

7.2.4 Impact of Evaporator and Condenser Effectiveness

Figures 14 (a) and (b) show the effect of evaporator and condenser effectiveness on the ECOP for both post and pre-cooling arrangements. The ECOP increases directly with the condenser and evaporator

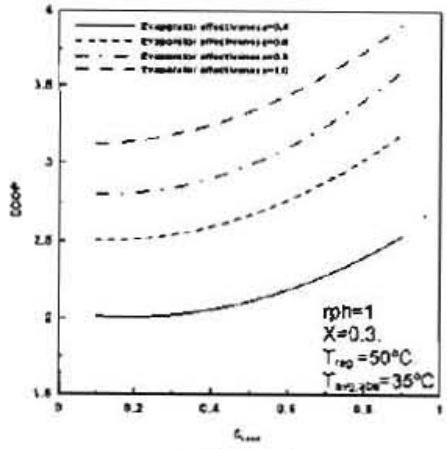

(a) Post-cooling

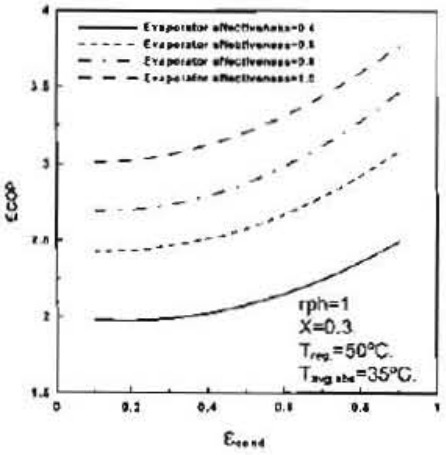

(b) Pre-cooling

Fig.14 Impact of evaporator and Condenser effectiveness on ECOP

effectiveness, as the condenser effectiveness increases the temperature of air exiting from it will be high and therefore the amount of additional heat required for regeneration for post-cooling arrangement will decrease, so the ECOP increases. At a condenser and evaporator effectiveness of 0.8 each the temperature of air exiting from the condenser is 52°C which is sufficient to regenerate the wheel in the pre-cooling arrangement. For the post-cooling arrangement the additional heat required at ε_{cond} of 0.8 is 0.52 kW for regeneration temperature of 60°C. While for ε_{cond} of 0.4 the regeneration energy will be 1.0 kW. For the evaporator, the increase of its effectiveness means lower temperature of air for the same cooling coil capacity. By increasing the ε_{ev} from 0.6 to 0.8, the specific cooling capacity of the supply air stream increases from 24.2 kJ/kg to 31.5 kJ/kg and then the system ECOP increases by about 16%.

7.2.5 Impact of Regeneration Air Temperature

Figures 15(a) and (b) show the impact of regeneration temperature on the ECOP for both post and pre-cooling arrangements. For post cooling arrangement, as the regeneration temperature increases the ECOP decreases. Although the increase of regeneration temperature enhances the desiccant wheel affinity to remove the latent load from air, this requires additional heating which lowers the ECOP. The energy required for regeneration at (V_{reg}= 2.5 m/s and T_{reg}= 80°C) is 1.15 kW and that at (V_{reg}= 2.5m/s and T_{reg}= 70°C) is 0.74 kW. So increasing T_{reg} from 70°C to 80°C will decrease the ECOP for post-cooling nearly by 15%. On the other hand the ECOP of the pre-cooling arrangement increases with regeneration air temperature. This is because the process air temperature is very low before entering to the desiccant wheel so, there is no need to regenerate the desiccant wheel at high temperature. The condenser heat is sufficient for regeneration process and hence there is no need for an auxiliary heater. Figure 15(c) shows the investigation of ECOP for both post and pre-cooling arrangements by changing the regeneration temperature beyond the operating ranges. At low regeneration temperature close

to 40°C, both systems have nearly the same values of ECOP. But at a regeneration temperature greater than 50°C, the ECOP of post cooling is enhanced by an amount of 10.4% compared to ECOP of pre-cooling.

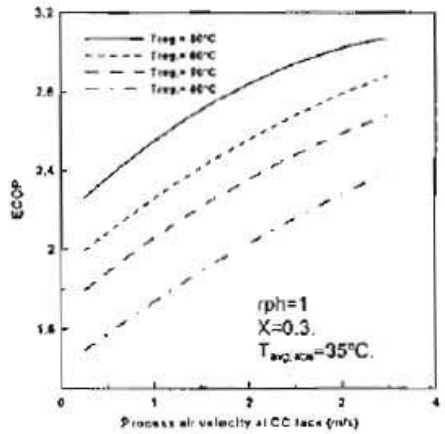

(a) Post-cooling

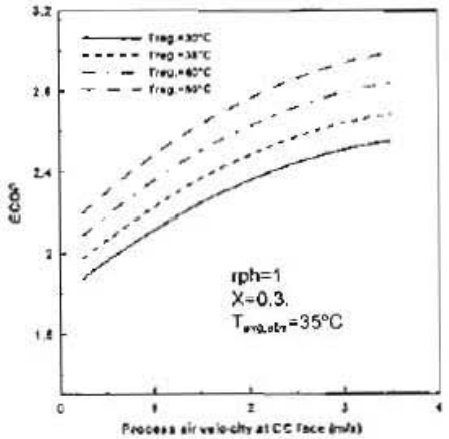

(b) Pre-cooling

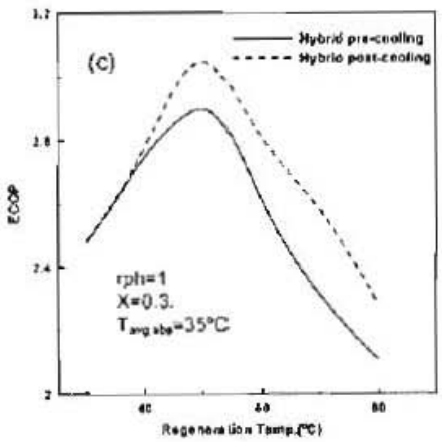

Fig.15 Impact of regeneration air temperature on ECOP

7.2.6 Impact of Regeneration Air Velocity

Figure 16(a) and (b) show the impact of regeneration air velocity on ECOP for both post and pre-cooling arrangements. For post cooling arrangement, as the regeneration velocity increases, the ECOP decreases because the increase in regeneration air velocity at constant regeneration temperature leads to high regeneration energy. The energy required for regeneration at (V_{reg}= 2.5 m/s and T_{reg}= 70°C) is 0.74 kW and that at (V_{reg}= 1.0 m/s and T_{reg}= 70°C) is 0.30 kW. So increasing V_{reg} from 1.0 m/s to 2.5 m/s will decrease the ECOP for post-cooling nearly by 8%. On the other hand the increasing of regeneration air velocity from 0.5 m/s to 1.5 m/s will increases the ECOP of the pre-cooling arrangement by about 17%.

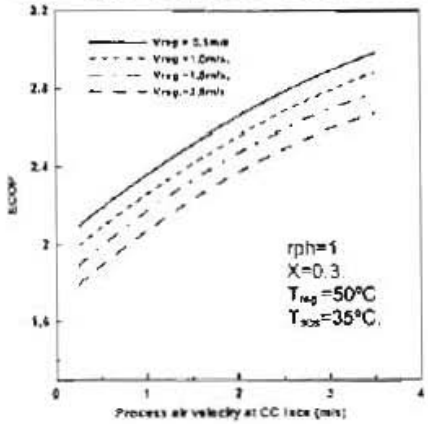

(a) Post-cooling

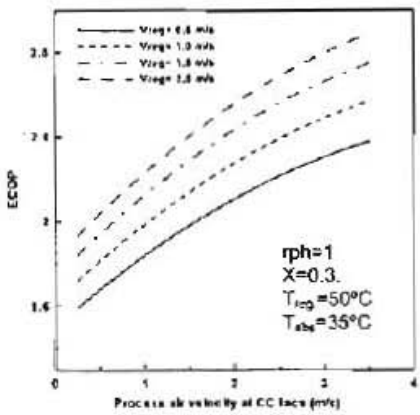

(b) Pre-cooling

Fig.16 Impact of regeneration air velocity on ECOP

7.3 The Hybrid Desiccant System and VCS

Figure 17 shows the COP for the hybrid system in post and pre-cooling arrangements; VCS and VCS with reheat. An auxiliary fan is used in the hybrid system only to supply air through the desiccant wheel. It is clear that the COP for each system increases with the mass flow rate because the supply air cooling capacity increases. The COP of the hybrid system in post-cooling mode has always higher values over the whole modes due to the latent load removed by dehumidification in the desiccant wheel before air passes through the cooling coil. This will decrease the compressor work required for post-cooling arrangement. An amount of 1.36 kW of compressor work is required for post-cooling arrangement compared to 2.27 kW required for pre-cooling arrangement. Also, the small compressor work of the post-cooling arrangement is referred to the use of the sensible heat exchanger (SHX). Figure 18 shows the variation of ECOP of post-cooling arrangement with and without SHX. It is shown that there is an enhancement in the ECOP of about 22% by using the SHX. The COP of the hybrid system in the pre-cooling mode has a value up to 80% greater than that of the VCS with reheat. This is because the reheat required to attains the same supply air conditions represents a penalty on the COP of the VCS. In the pre-cooling arrangement, the process air enters to the cooling coil then passes over the desiccant wheel i.e. the total latent and sensible loads are removed by the cooling coil. So, the value of COP of pre-cooling is lower than that of post-cooling by about 12.5%. The

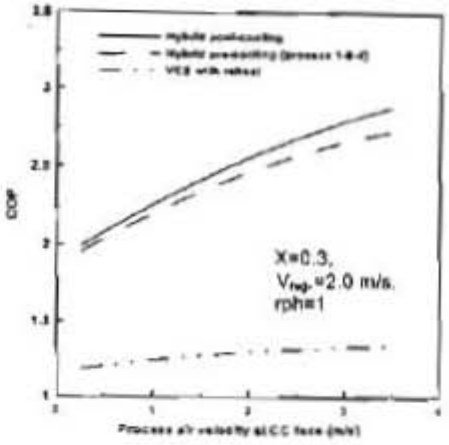

Fig. 17 Variation of COP with process air velocity

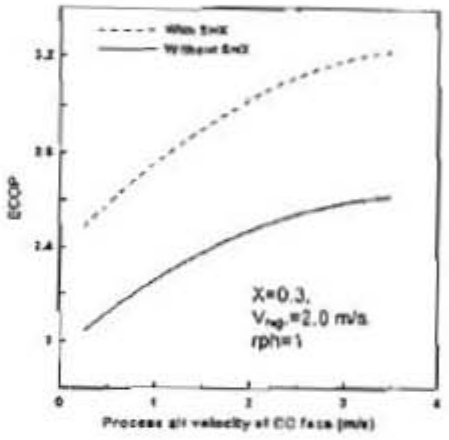

Fig. 18 Variation of ECOP of post-cooling mode with and without SHX.

value of COP of VCS with reheat is nearly 50% of that of post cooling hybrid system.

Figure 19 shows that the specific moisture removing rate (SMRR) for the pre-cooling hybrid desiccant mode reached higher values than other systems and this explains why this system has the lower dew point temperature as shown in Fig. 20. After air exiting from the cooling coil in the pre-cooling arrangement, it is further dehumidified to lower values by passing through the desiccant wheel. It is very difficult to reach the same degree of humidity by the VCS because moisture may be frozen on the evaporator surface as a result of deep cooling. The pre-cooling

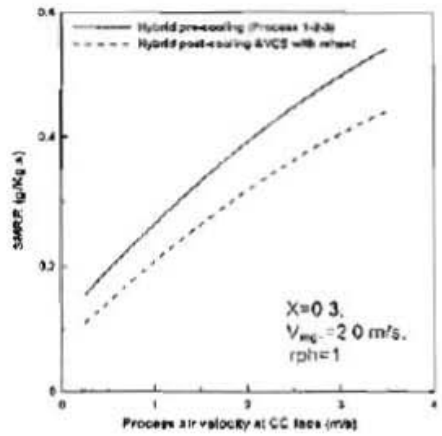

Fig. 19 Variation of SMRR with process air velocity

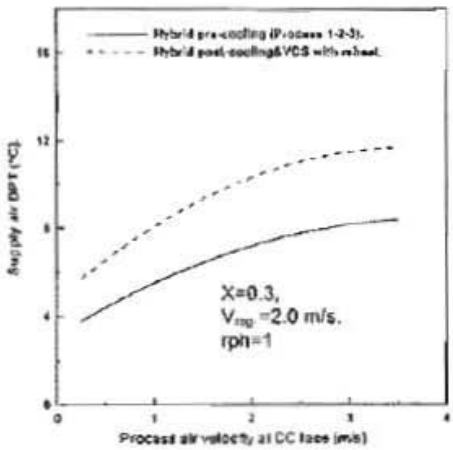

Fig. 20 Variation of supply air DPT with process air velocity.

mode is usually used when the design supply air dew point temperature is very low (less than 6°C) and it is also used for controlling the relative humidity which is an important measure of maintaining good IAQ.

Fig. 21 shows the variation of dry bulb temperature (DBT) and achieved heat ($Q_{ach.}$) for the different systems, the pre-cooling mode has a DBT higher than that of VCS due to the sensible heat gain from the dehumidification of process air after leaving the cooling coil. The sensible heat rise here is significant as it leads to further lowering in DPT and moisture content of the process air which helps in humidity and temperature control. Fig. 21 explains the previous analysis, it can be seen that the achieved heat from the pre-cooling system is found to be 0.65 to 1.5 kW compared to the reheat system which requires 2 kW to achieve the same sensible heat factor.

Fig. 22 shows the cooling coil capacity and energy saving percent. The post-cooling mode has less cooling coil capacity than the pre-cooling and the VCS. Then the use of post-cooling mode results in an energy saving in the order of 25%-30%, this saving will reduce the size of the VCS incorporated with the desiccant system. So the post-cooling hybrid desiccant system is a cost-effective one for air conditioning system with better performance.

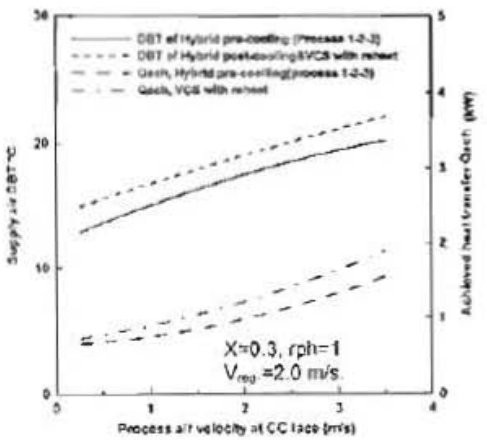

Fig. 21 Variation of DBT and $Q_{ach.}$ with process air velocity.

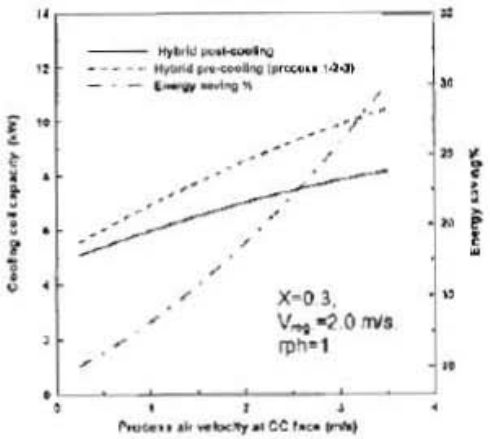

Fig. 22 Cooling coil capacity Percent of energy saving with process air velocity

Conclusion

A theoretical model to predict the performance of the hybrid desiccant system is introduced and solved. A desiccant wheel impregnated with lithium chloride as the working desiccant which is considered the heart of the hybrid desiccant system has been developed. This model is numerically validated by comparing its results with other published model. A small rotational speed close to 1 rph are required for the best performance of the desiccant wheel, the specific moisture removal rate is found to be 0.28 g/kg.s at these values. As the regeneration area increases the temperature of the regeneration air stream will decreases, the regeneration temperature is 60°C at regeneration to absorption area ratio of unity. A higher thermal capacitance ratio is recommended for better wheel performance. A comparison between the different configurations of the hybrid desiccant system and the VCS show that:

- The post cooling hybrid desiccant system has the higher COP, nearly twice that of VCS with reheat which ensures an energy saving of the cooling coil capacity up to 30% for the same cooling effect.
- The post cooling and pre cooling ensures better IAQ with an increase of about 80% in the COP for the pre cooling mode compared to VCS with reheat.
- The pre cooling mode has the maximum SMRR in all the systems, so it supplies air at lower dew point temperature (6°C). The pre cooling mode is usually used for easily controlling the indoor air conditions especially for lower humidity ratio levels, but the post cooling mode can be used to save energy consumption.
- A moderate void fraction area of 0.4 with a suitable desiccant surface area to volume ratio of 1600 is recommended for the best performance.
- A suitable choice for the regeneration air temperature and velocity is very important to ensure best performance.
- The higher the effectiveness of dehumidification, evaporator and condenser the higher is the ECOP.

References

1. Zhang L.z., j.l. Niu, "A pre-cooling Munters environmental control desiccant cooling cycle with chilled-ceiling panel," Enegy 28 (2003), PP.275-292.
2. Dunkle, R.V., "A method of solar air conditioning " Mech. and Chem. Eng. Trans., Inst. Eng. Austeralia, MCI, Vol. 73 MAY 1975.
3. Close D.J and Sheridan, J. C, " Low energy cooling for humid regions." Australian institute of refrigeration air conditioning and heating, (AIRAH) Federal conference, Tasmania, 1982.
4. Sheridan, J. C. and mitchell, J. W, "Hybrid solar desiccant cooling systems", proceeding of the 1982 annual meeting of AS/ISES, 1982.
5. Robert, R.H, "Model and performance characteristics of a commercially sized hybrid air conditioning system which utilizes rotary desiccant dehumidifier," PhD Wisconsin university; 1983.
6. Burns P.R., J.W. Mitchell, W.A.Beckman, "Hybrid desiccant

cooling systems in super market applications", ASHRAE Trans 91 (Part-1B) (1985) 457-468.

7. Maclaine-Cross I.L., "Hybrid desiccant cooling in Australia", Australian Refrigeration Air-conditioning and Heating 41 (5) (1987) 16-25.
8. Worek W.M., C.J. Moon, "Desiccant integrated hybrid vapor compression cooling - performance sensitivity to outdoor conditions", Heat Recovery Systems and CHP 8 (6) (1988) 489-501.
9. Singh S.K., S. Jain, S.C. Kaushik, "Energy conservation through hybrid air conditioning cycles: computer modelling studies", technical report, I.I.T. Delhi, 1996.
10. Vazirifard S., M. H. Saidi, "hybrid desiccant cooling systems " Published in ASHRAE Journal Vol. 49, Jan. 2006.
11. Mohan B. Shaji, Prakash Maiya M. and Shaligram Tiwar," Performance characterisation of liquid desiccant columns for a hybrid air-conditioner". Applied Thermal Engineering 28 (2008) 1342–1355.
12. Zhang X.J., Dai Y. J. and R.Z. Wang, , "A simulation study of heat and mass transfer in a honeycombed rotary desiccant dehumidifier," Appl. therm. Eng. 23, pp. 989-1003, 2003.
13. Ahmed M. Hamed, A. Khalil, A.E. Kabeel, M.M. Bassuoni and A.M. Elzahaby, "Performance analysis of dehumidification rotating wheel using liquid desiccant.", Renewable Energy 30 (2005) 1689–1712.
14. Dai Y. J., R.Z. Wang, and, H.F. Zhang, "Parameter Analysis to Improve Rotary Desiccant Dehumidification Using a Mathematical Model," Int. J. Therm. Sci. 40, pp. 400-408,2001.